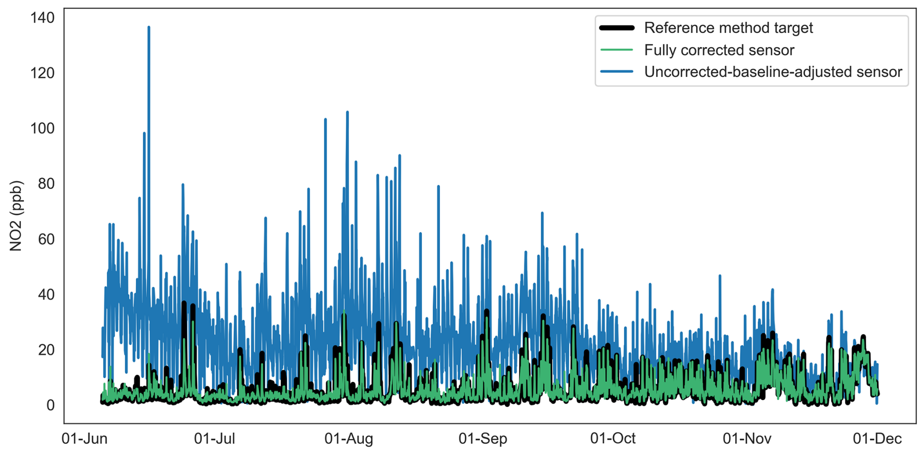

Figure 9. Time series of uncorrected-baseline-adjusted sensor, fully corrected sensor and reference method observations for NO_2 at Oxford St Ebbe's for 2020.

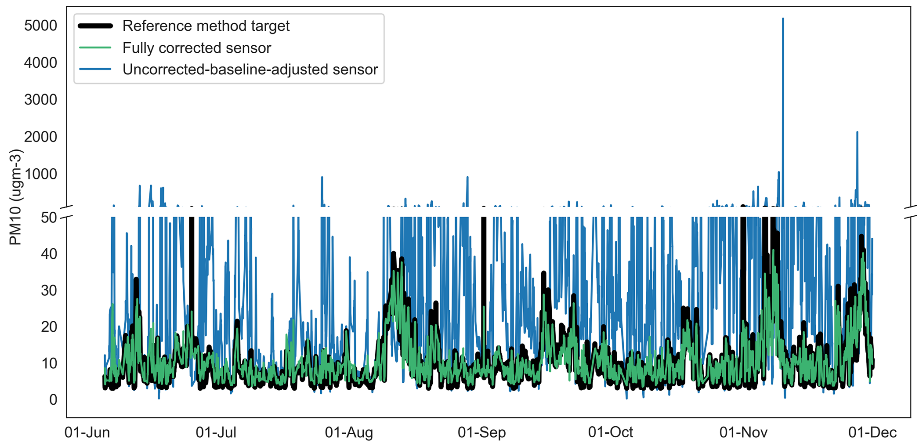

Figure 10. Time series of uncorrected-baseline-adjusted sensor, fully corrected sensor and reference method observations for PM_{10} at Oxford St Ebbe's for 2020. ugm-3: $\mu g\,m^{-3}$.

servations, e.g. at most 15 min means, is essential for effectively screening transient anomalous sensor behaviours which skew sensor datasets significantly and mask important underlying data structures or anomalies. We also note that the reference method data-resolved to these time resolutions is difficult to obtain in the UK.

3.3 Random forest correction modelling results

3.3.1 Random forest regression model training

Outputs from the model training exercise are shown in Figs. 6–8 as a series of regression plots for the RFR models developed for NO_2, PM_{10} and $PM_{2.5}$. For each pollutant, three regression plots are presented to illustrate (i) the relationship between the baseline-corrected sensor observations and reference method (left), (ii) the same relationship constrained to the validation subset (middle), and (iii) the relationship between the fully corrected sensor observations (with both baseline correction and RFR interference corrections applied) and reference method. A simple ordinary least-squares (OLS) regression analysis is presented in each case to describe each relationship. All data shown are at a 15 min mean resolution.

The plots to the right of Figs. 6–8 show that the respective RF models are highly effective in predicting the target observations (reference method). In doing so, they demonstrate their capability to predict the combined interferences from a variety of environmental factors found in the data of the left and middle regression plots. The left and middle plots also show that training and validation datasets come from the same sample population (one having been randomly sampled from the other), providing a useful internal validation of model training to reflect variations in training features. Further checks on the models using unseen data from outside of the sample populations will better test likely performance of the models in the field.

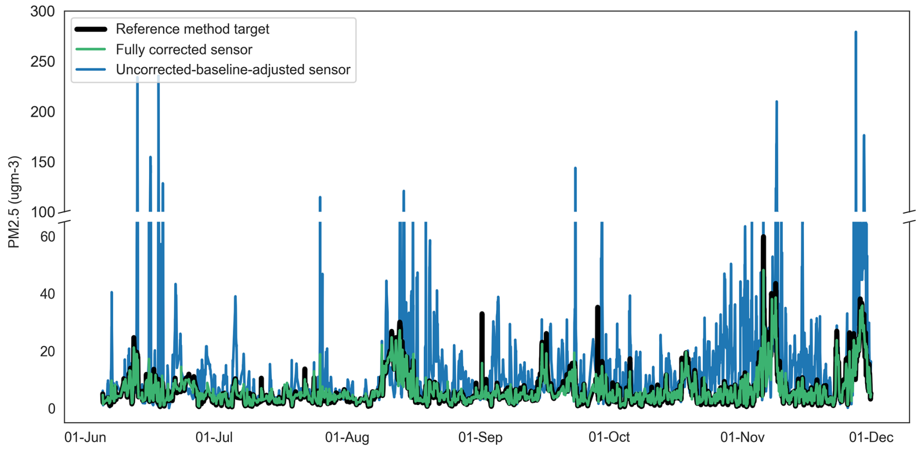

Figure 11. Time series of uncorrected-baseline-adjusted sensor, fully corrected sensor and reference method observations for $PM_{2.5}$ at Oxford St Ebbe's for 2020. ugm-3: $\mu g\,m^{-3}$.

Table 4. RFR correction model performance in terms of the MAE relative to reference method observations (validation data) for June to November 2020.

	Mean absolute error (MAE)		Coefficient of determination (R^2)		Change in the MAE arising from full RFR correction
	Baseline corrected	Fully corrected (baseline + RFR)	Baseline corrected	Fully corrected (baseline + RFR)	
NO_2 (ppb)	16.8	1.2	0.05	0.86	93 %
PM_{10} ($\mu g\,m^{-3}$)	34.6	1.9	0.01	0.79	95 %
$PM_{2.5}$ ($\mu g\,m^{-3}$)	8.9	0.9	0.28	0.91	90 %

Figures 6–8 show the dramatic impact of the RF model correction as demonstrated by the coefficients of variation in each of the three cases. The R^2 value of the fully corrected sensor vs. reference method observations is a convenient evaluator for the ability of the models to capture the variability in the dependent datasets. Clearly, the $PM_{2.5}$ model performs excellently in this respect with an R^2 value of 0.91 and OLS slope and intercept terms approaching unity. The respective R^2 value for both PM_{10} and NO_2 RF models (0.79 and 0.86) also indicate good model performance. The values for R^2 above are consistent with the out-of-bag scores achieved at training time (0.85, 0.79 and 0.91 for NO_2, PM_{10}, and $PM_{2.5}$ respectively) which provide an additional check on model performance using data not explicitly used in the training. Even so, it is clear from Figs. 6 and 7 that the models struggled, on occasion, to accurately predict higher reference concentrations, and NO_2 and PM_{10} predicted concentrations are generally more scattered compared with $PM_{2.5}$. It is also noticeable that in all three cases the RF models are biased, tending to underpredict the reference concentration as demonstrated by the regression equation slope terms, and this is particularly noticeable in the > 15 ppb concentration unit range.

3.3.2 RF correction performance characteristics (hold-out validation set)

The performance of each component of the correction method upon 15 min mean data is presented in Table 4 in terms of the MAE delivered by correction outputs at each stage, relative to the reference method observations. Table 4 shows that the RFR correction adds significant value to the baseline correction, alone contributing to a further 90 %–95 % reduction in the MAE terms. In concentration units this equates to fully corrected NO_2 sensor observations within approximately ± 1.2 ppb of the reference observation. Similar comparisons for PM_{10} and $PM_{2.5}$ indicate fully corrected concentrations within $\pm 0.9\,\mu g\,m^{-3}$ (PM_{10}) and $1.9\,\mu g\,m^{-3}$ ($PM_{2.5}$) of the reference method. These compare favourably with results in the literature for all three pollutants.

The impact of corrections to this order of magnitude upon the sensor time series can be visualised in Figs. 9–11, which present 15 min mean uncorrected-baseline-adjusted sensor observations, fully corrected sensor observations and reference observations for NO_2, PM_{10} and $PM_{2.5}$. Figure 9 shows that for NO_2 there is some visual evidence of the RFR model overcorrecting (relative to the reference method) during periods of peak concentration, particularly in mid to late June

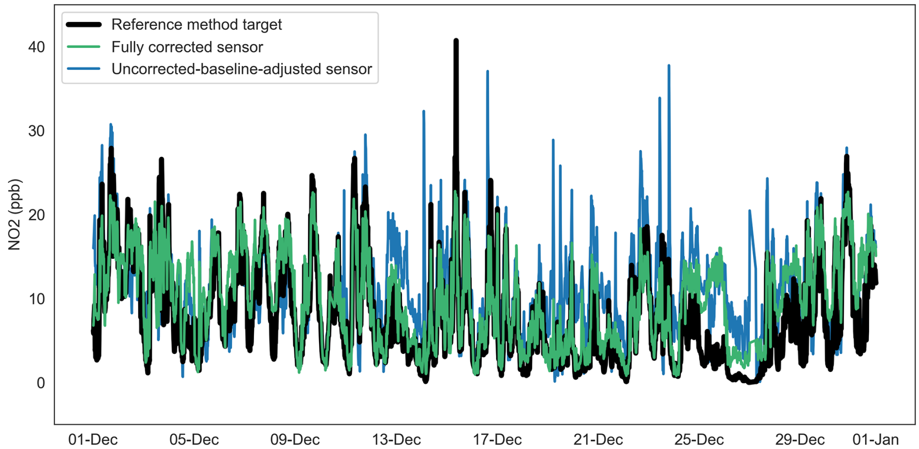

Figure 12. Time series of uncorrected-baseline-adjusted sensor, fully corrected sensor and reference method observations for NO_2 at Oxford St Ebbe's (unseen data) for December 2020.

Table 5. RFR correction model performance in terms of the MAE relative to reference method observations (unseen data) for December 2020.

	Mean absolute error (MAE)		Change in the MAE arising from
	Baseline corrected	Fully corrected (baseline + RFR correction)	full RFR correction
NO_2 (ppb)	4.1	2.6	37 %
PM_{10} ($\mu g\, m^{-3}$)	75.5	4.4	94 %
$PM_{2.5}$ ($\mu g\, m^{-3}$)	10.0	2.7	73 %

and August. Otherwise, the NO_2 correction tracks that of the reference observations well.

3.3.3 RF correction model performance characteristics (unseen data)

Table 5 presents estimates of the correction model performance based on 15 min mean unseen data from December 2020, i.e. data used previously for neither model training nor validation. The data shown are, as expected, less favourable compared with the validation set, returning higher values for the MAE metric, but for the air quality context, these values are within 1.4 ppb (NO_2) and 2.5 $\mu g\, m^{-3}$ (PM_{10}) and 1.8 $\mu g\, m^{-3}$ ($PM_{2.5}$) of the MAE returned by the model validation set (Tables 4 and 5).

In late November–December 2020 and latterly, continuing through the first quarter of 2021 (not shown), the sensor network observed episodes of high particle concentrations which coincided with a drop in ambient temperature (and dew point temperature) to the order of 10 °C. Neither reciprocal changes in relative humidity were observed, nor was there an obvious change in sensor sample flow rate. It is noteworthy also that similar conditions were not commonplace throughout the model training dataset (June to November 2020). The episode conditions observed by the sensor network were not replicated in the reference method dataset and are likely the main driver for the increase in the MAE for the particulate matter correction models shown in Table 5. Figures 13–14 show examples of the episodes in December 2020 for PM_{10} and $PM_{2.5}$ respectively, including the absence of a reciprocal peak in the reference data and the performance of the model correction.

Despite these issues, and as demonstrated in Figs. 13–14, the RF models deliver substantial improvements on the raw dataset (not shown in Table 5) and baseline-adjusted data (shown). Improvements in the MAE attributable to the RF model in the range of 37 %–94 % are shown; these are equivalent to fully corrected observations within, on average, approximately ±2.6 ppb of the reference method for NO_2, ±4.4 $\mu g\, m^{-3}$ for PM_{10} and ±2.7 $\mu g\, m^{-3}$ for $PM_{2.5}$.

The decrease in model performance observed with the unseen dataset and the observations on ambient conditions and sensor operation (above) illustrate the need for long time series for model training, covering all environmental conditions to which the sensors will be exposed.

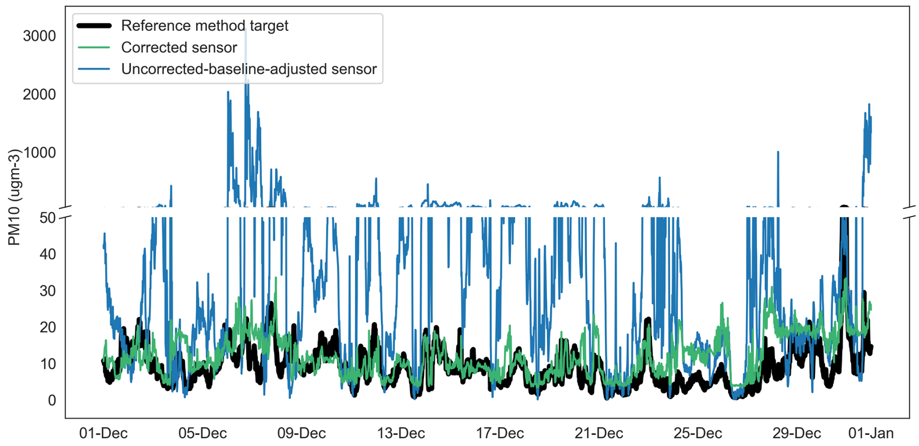

Figure 13. Time series of uncorrected-baseline-adjusted sensor, fully corrected sensor and reference method observations for PM_{10} at Oxford St Ebbe's (unseen data) for December 2020. ugm-3: $\mu g\,m^{-3}$.

Table 6. Expanded-uncertainty estimates for fully corrected sensor observations using the RFR validation dataset (the target values are the target expanded-uncertainty criteria recommended by European legislation).

Pollutant	Expanded uncertainty	Fully and finally corrected expanded uncertainty*	R^2 value	Conformance with target expanded-uncertainty objective
NO_2	21 %	17 %	0.86	True, ≤ 25 %
PM_{10}	40 %	15 %	0.79	True, ≤ 50 %
$PM_{2.5}$	19 %	12 %	0.91	True, ≤ 50 %

* Expanded-uncertainty estimates with allowance to correct for a non-zero intercept and non-unitary slope in the linear regression relationship of the sensor to the reference method.

3.3.4 Corrected sensor performance vs. European air quality data quality objectives

Tables 6 and 7 present expanded-uncertainty estimates for fully corrected sensor observations. These estimates were calculated using a spreadsheet tool (EC Working Group, 2020) to provide a further performance indicator on the adequacy of these data for air quality assessment applications. Table 6 presents expanded-uncertainty estimates associated with fully corrected sensor data from the validation dataset (data not used in the RFR model training) and shows that these data for all pollutants perform well against the target expanded-uncertainty criteria recommended by European legislation (expanded uncertainties of 21 %, 40 % and 19 % respectively for NO_2, PM_{10} and $PM_{2.5}$). Guidance on the calculation of expanded uncertainty (EC Working Group, 2010) also allows for the correction of slope and intercept terms in the relationship between the sensor and reference method. The result of this further correction is presented in Table 6 as the "full and final correction". Expanded-uncertainty estimates for the validation set with full and final corrections applied were 17 %, 15 % and 12 % for NO_2, PM_{10} and $PM_{2.5}$ respectively. Highly respectable coefficients of determination between reference and fully and finally corrected sensor observations were also found in all cases as already shown in Figs. 6–8. However, because the validation set and model training datasets are closely coupled – the validation set being taken at random from the same sample population as that used for model training – expanded-uncertainty estimates based solely on these data should be interpreted with caution and may, depending on the application scenario of the correction model, present an overly optimistic estimate of real-world measurement uncertainty.

Results from reciprocal calculations based on unseen data offer a more rigorous/precautionary test of expanded uncertainty, indicative of real-world applications. Table 7 presents these data for fully corrected sensor observations from December 2020. Table 7 shows the expanded-uncertainty estimates for fully corrected unseen sensor data of 29 %, 21 % and 27 % respectively for NO_2, PM_{10} and $PM_{2.5}$. Further corrections, for slope and intercept terms, had negligible change on these estimates (30 %, 25 % and 28 % expanded uncertainty respectively for NO_2, PM_{10} and $PM_{2.5}$). As expected, these data are more uncertain than the validation set; even so, performance is good relative to the target data quality objectives (DQOs). The fully and finally corrected datasets for PM_{10} and $PM_{2.5}$ meet the expanded-uncertainty criteria recommended by European legislation. The expanded-

Table 7. Expanded-uncertainty estimates for fully corrected sensor observations from an unseen dataset for December 2020 (the target values are the target expanded-uncertainty criteria recommended by European legislation).

Pollutant	Expanded uncertainty	Fully and finally corrected expanded uncertainty*	R^2 value	Conformance with target expanded-uncertainty objective
NO_2	29 %	30 %	0.72	False, ≤ 25 %
PM_{10}	21 %	25 %	0.30	True, ≤ 50 %
$PM_{2.5}$	27 %	28 %	0.47	True, ≤ 50 %

* Expanded-uncertainty estimates with allowance to correct for a non-zero intercept and non-unitary slope in the linear regression relationship of the sensor to the reference method.

uncertainty estimate for NO_2 was within 5 % of the acceptance criteria.

4 Conclusions

This study has presented and demonstrated a simple and effective method for attenuating the confounding effects of sensor baseline variability and interferences from ambient environmental parameters upon low-cost electrochemical and optical particle counter sensor signals.

The methods presented in this paper have been tested at a high temporal resolution against high-quality, co-located reference method observations sourced from the UK's regulatory monitoring network (AURN). Using the MAE as an indicator of sensor error (relative to reference observations), the methods developed can reduce the error in NO_2, PM_{10} and $PM_{2.5}$ observations from the low-cost sensors tested by up to 88 %–95 % (based on model validation data not used in RF training). In the case of the low-cost NO_2 sensor, corrections reduced the MAE of sensor observations to within ±1.2 ppb of the reference observation. Similarly, for PM_{10} and $PM_{2.5}$, MAE estimates were within ±1.9 and ±0.9 $\mu g\, m^{-3}$ respectively. The R^2 value achieved for fully corrected NO_2, PM_{10} and $PM_{2.5}$ sensor observations were 0.86, 0.79 and 0.91 respectively.

Tests on how the methods generalised to unseen conditions have shown that the RFR correction models trained on data from June to November 2020 are tolerant of a wide range of competing environmental interferences. Tests based on data from December 2020, unseen by the RF model in training, delivered MAE estimates for fully corrected low-cost NO_2, PM_{10} and $PM_{2.5}$ sensors of 2.6 ppb, 4.4 and 2.7 $\mu g\, m^{-3}$ respectively. Despite this observed (and expected) drop in performance, the MAE values in corrections to unseen datasets were within 1.4 ppb (NO_2) and 2.5 $\mu g\, m^{-3}$ (PM_{10}) and 1.8 $\mu g\, m^{-3}$ ($PM_{2.5}$) of those returned by the model validation set.

Given these indicators for the level of improved uncertainty that can be achievable with the methods presented, we propose that data from reputable, high-quality sensors may now have a meaningful role in the air quality assessment toolkit. Indeed, using the methods presented, sensor data may deliver data quality of at least comparable levels to that displayed by passive sampler methods (for NO_2), with the benefit of higher temporal resolution.

To substantiate potential future applications, this paper has presented data demonstrating that the RF-based methods are capable of delivering fully corrected low-cost sensor data that meet the general requirements for "indicative measurements" as set out by the European Ambient Air Quality Directive. In doing so, we have used methods prescribed by the European Commission Working Group on Guidance for the Demonstration of Equivalence to calculate expanded-uncertainty estimates for fully corrected sensor observations. For tests based on validation and unseen datasets, the expanded uncertainty of fully corrected sensor data was within the requirements set by the European Ambient Air Quality Directive for indicative monitoring (within ±25 % of the reference observation for NO_2, ±50 % for particles) for PM_{10} and $PM_{2.5}$. Estimates for NO_2 were outside of the acceptance criteria by ∼ 5 %. Fully corrected expanded-uncertainty estimates for PM_{10} and $PM_{2.5}$ were within or proximal to the equivalence thresholds (±25 %) established by the European Commission Working Group on Guidance for the Demonstration of Equivalence. In tests using unseen data, the most stringent test available to the study, the expanded-uncertainty estimates for RFR-model-corrected observations for NO_2, PM_{10} and $PM_{2.5}$ were 30 %, 25 % and 28 % respectively.

Demonstrating conformance with these regulatory thresholds in a traceable way is a significant milestone, not only for the potential to unlock applications as "supplementary assessment" methods for compliance assessments but also within the context of the stringency of the acceptance criteria and the rigour of the expanded-uncertainty calculation method set out by the working group.

We anticipate application of the model in other local contexts will require re-training and validation of the RF model for local conditions, an important focus for future research. As such, the techniques developed are presented as a working method to be adapted for other applications rather than a definitive model for wider generalisations. We also note that scaling of the method to applications across a sensor network is likely to be limited by the diversity of the RF training

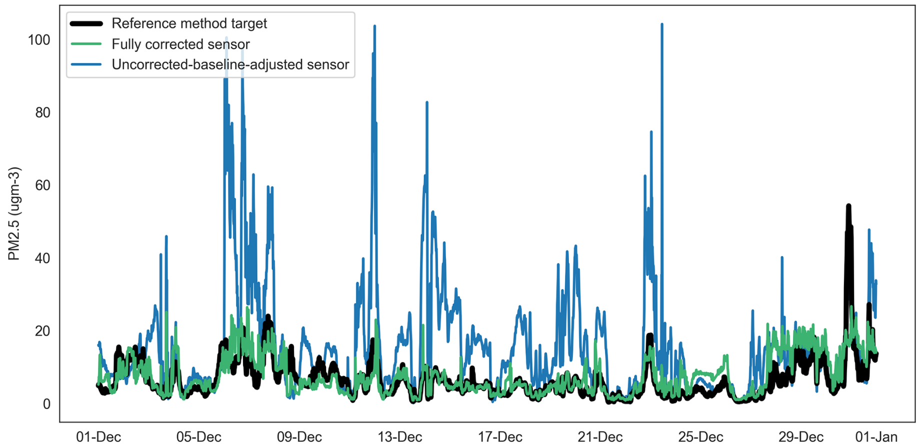

Figure 14. Time series of uncorrected-baseline-adjusted sensor, fully corrected sensor and reference method observations for $PM_{2.5}$ at Oxford St Ebbe's (unseen data) for December 2020. ugm-3: $\mu g\, m^{-3}$.

datasets and the quality of the city scale background (both spatial and scalar representativeness). However, this work has demonstrated capabilities for applications to monitoring across a small city, with clear potential benefits for supporting air quality management.

Code availability. Code arising from this study is being prepared for deposit in the UK Natural Environment Research Council (NERC) Centre for Environmental Data Analysis (CEDA) Archive at https://www.ceda.ac.uk/services/ceda-archive/ (CEDA Archive, 2022). Prior to deposit in CEDA, data are available from the corresponding authors upon request.

Data availability. Reference measurement datasets at 15 min resolution were sourced from Ricardo Energy & Environment, Harwell, UK (Brian Stacey, personal communication, throughout 2020–2021). Reference measurement datasets at 1 h resolution were sourced from https://uk-air.defra.gov.uk/data/ (Defra, 2022). Sensor datasets arising from this study are being prepared for deposit in the UK Natural Environment Research Council (NERC) Centre for Environmental Data Analysis (CEDA) Archive at https://www.ceda.ac.uk/services/ceda-archive/ (CEDA Archive, 2022). Prior to deposit in CEDA, data are available from the corresponding authors upon request.

Author contributions. FL, NP, SB and TB conceived the study. TB and FL corralled the data. TB and NP performed data analysis. BS supplied reference observations at the required resolutions and finessed expanded-uncertainty estimates in accordance with the guidance. TB drafted the paper. All co-authors contributed to reviewing and editing the paper.

Competing interests. At least one of the (co-)authors is a member of the editorial board of *Atmospheric Measurement Techniques*. The peer-review process was guided by an independent editor, and the authors also have no other competing interests to declare.

Acknowledgements. The authors would like to extend thanks and gratitude to the chair of the project steering committee, the late Martin Williams, for his guidance and encouragement over the years. The authors would also like to thank the study steering group for their technical contributions and administrative support and Ricardo Energy & Environment for facilitating data acquisition. Oxford City Council and Oxfordshire County Council are both thanked for advice and support.

Financial support. This research was funded by the Natural Environment Research Council (grant no. NE/V010360/1). Its forerunning pilot project was funded by the National Institute for Health and Care Research (NIHR130095; NIHR Public Health Research). The views expressed are those of the author(s) and not necessarily those of the NIHR or the Department of Health and Social Care. This publication arises in part from research funded by Research England's Strategic Priorities Fund (SPF) quality related (QR) allocation.

Review statement. This paper was edited by Pierre Herckes and reviewed by two anonymous referees.

References

Alphasense Ltd.: NO2-A43F Nitrogen Dioxide Sensor 4-Electrode Technical Specification, https://www.alphasense.com/wp-content/uploads/2019/09/NO2-A43F.pdf (last access: 19 May 2021), 2019a.

Alphasense Ltd.: OPC-N3 Particle Monitor Technical Specification, https://www.alphasense.com/wp-content/uploads/2019/03/OPC-N3.pdf (last access: 19 May 2021), 2019b.

Berrar, D.: Cross-validation, in Encyclopaedia of Bioinformatics and Computational Biology: ABC of Bioinformatics, Elsevier, 3, 542–545, 2018.

Bigi, A., Mueller, M., Grange, S. K., Ghermandi, G., and Hueglin, C.: Performance of NO, NO_2 low cost sensors and three calibration approaches within a real world application, Atmos. Meas. Tech., 11, 3717–3735, https://doi.org/10.5194/amt-11-3717-2018, 2018.

Breiman, L.: Bagging predictors, Mach. Learn., 24, 123–140, https://doi.org/10.1023/A:1018054314350, 1996.

Breiman, L.: Random forests, Mach. Learn., 45, 5–32, https://doi.org/10.1023/A:1010933404324, 2001.

Castell, N., Dauge, F. R., Schneider, P., Vogt, M., Lerner, U., Fishbain, B., Broday, D., and Bartonova, A.: Can commercial low-cost sensor platforms contribute to air quality monitoring and exposure estimates?, Environ. Int., 99, 293–302, https://doi.org/10.1016/j.envint.2016.12.007, 2017.

CEDA: CEDA Archive, STFC, UK, CEDA [code, data set], https://www.ceda.ac.uk/services/ceda-archive/, last access: 24 May 2022.

Clements, A. L., Reece, S., Conner, T., and Williams, R.: Observed data quality concerns involving low-cost air sensors, Atmos. Environ., 3, 100034, https://doi.org/10.1016/j.aeaoa.2019.100034, 2019.

Crilley, L. R., Shaw, M., Pound, R., Kramer, L. J., Price, R., Young, S., Lewis, A. C., and Pope, F. D.: Evaluation of a low-cost optical particle counter (Alphasense OPC-N2) for ambient air monitoring, Atmos. Meas. Tech., 11, 709–720, https://doi.org/10.5194/amt-11-709-2018, 2018.

Crilley, L. R., Singh, A., Kramer, L. J., Shaw, M. D., Alam, M. S., Apte, J. S., Bloss, W. J., Hildebrandt Ruiz, L., Fu, P., Fu, W., Gani, S., Gatari, M., Ilyinskaya, E., Lewis, A. C., Ng'ang'a, D., Sun, Y., Whitty, R. C. W., Yue, S., Young, S., and Pope, F. D.: Effect of aerosol composition on the performance of low-cost optical particle counter correction factors, Atmos. Meas. Tech., 13, 1181–1193, https://doi.org/10.5194/amt-13-1181-2020, 2020.

Cross, E. S., Williams, L. R., Lewis, D. K., Magoon, G. R., Onasch, T. B., Kaminsky, M. L., Worsnop, D. R., and Jayne, J. T.: Use of electrochemical sensors for measurement of air pollution: correcting interference response and validating measurements, Atmos. Meas. Tech., 10, 3575–3588, https://doi.org/10.5194/amt-10-3575-2017, 2017.

Defra: Quality Assurance and Quality Control (QA/QC) Procedures for UK Air Quality Monitoring under 2008/50/EC and 2004/107/EC, https://uk-air.defra.gov.uk/assets/documents/reports/cat09/1902040953_All_Networks_QAQC_Document_2012__Issue2.pdf (last access: 5 May 2021), 2013.

Defra: Clean Air Strategy 2019, https://www.gov.uk/government/publications/clean-air-strategy-2019 (last access: 24 May 2022), 2019.

Defra: Site Information for Oxford St Ebbes(UKA00518) – Defra, UK, https://uk-air.defra.gov.uk/networks/site-info?uka_id=UKA00518&provider=, last access: 21 April 2021.

Defra: UK Air Information Resource – Defra, UK [data set], https://uk-air.defra.gov.uk/data, last access: 24 May 2022.

Defra and DfT: UK plan for tackling roadside nitrogen dioxide concentrations: An overview, https://www.gov.uk/government/publications/air-quality-plan-for-nitrogen-dioxide-no2-in-uk-2017 (last access: 24 May 2022), 2017.

EC Working Group: Guide to the demonstration of equivalence of ambient air monitoring methods Report by an EC Working Group on Guidance for the Demonstration of Equivalence, https://ec.europa.eu/environment/air/quality/legislation/pdf/equivalence.pdf (last access: 24 May 2022), 2010.

EC Working Group: Equivalence Spreadsheet Tool on the Demonstration of Equivalence, Version Control, Version 3.1, 02/07/20, https://ec.europa.eu/environment/air/quality/legislation/pdf/EquivalenceTool%20V3.1%20020720.xlsx (last access: 5 May 2021), 2020.

Esposito, E., De Vito, S., Salvato, M., Bright, V., Jones, R. L., and Popoola, O.: Dynamic neural network architectures for on field stochastic calibration of indicative low-cost air quality sensing systems, Sensor. Actuat. B-Chem., 231, 701–713, https://doi.org/10.1016/j.snb.2016.03.038, 2016.

Hasenfratz, D., Saukh, O., and Thiele, L.: On-the-Fly Calibration of Low-Cost Gas Sensors, in Wireless Sensor Networks, edited by: Picco, P. G. and Heinzelman, W., Springer Berlin Heidelberg, Berlin, Heidelberg, 228–244, 2012.

Hastie, T., Tibshirani, R., and Friedman, J.: The Elements of Statistical Learning, https://doi.org/10.1007/978-0-387-84858-7, 2009.

Karagulian, F., Barbiere, M., Kotsev, A., Spinelle, L., Gerboles, M., Lagler, F., Redon, N., Crunaire, S., and Borowiak, A.: Review of the performance of low-cost sensors for air quality monitoring, Atmosphere, 10, 506, https://doi.org/10.3390/atmos10090506, 2019.

Kelly, F. P.: Associations of long-term average concentrations of nitrogen dioxide with motality, COMEAP Report, https://assets.publishing.service.gov.uk/government/uploads/system/uploads/attachment_data/file/734799/COMEAP_NO2_Report.pdf (last access: 24 May 2022), 2018.

Leach, F. C. P., Peckham, M. S., and Hammond, M. J.: Identifying NO_x Hotspots in Transient Urban Driving of Two Diesel Buses and a Diesel Car, Atmosphere, 11, 355, https://doi.org/10.3390/atmos11040355, 2020.

Lim, C. C., Kim, H., Vilcassim, M. J. R., Thurston, G. D., Gordon, T., Chen, L. C., Lee, K., Heimbinder, M., and Kim, S. Y.: Mapping urban air quality using mobile sampling with low-cost sensors and machine learning in Seoul, South Korea, Environ. Int., 131, 105022, https://doi.org/10.1016/J.ENVINT.2019.105022, 2019.

Morawska, L., Thai, P. K., Liu, X., Asumadu-Sakyi, A., Ayoko, G., Bartonova, A., Bedini, A., Chai, F., Christensen, B., Dunbabin, M., Gao, J., Hagler, G. S. W., Jayaratne, R., Kumar, P., Lau, A. K. H., Louie, P. K. K., Mazaheri, M., Ning, Z., Motta, N., Mullins, B., Rahman, M. M., Ristovski, Z., Shafiei, M., Tjondronegoro, D., Westerdahl, D., and Williams, R.: Applications of low-cost sensing technologies for air quality monitoring and exposure assessment: How far have they gone?, Environ. Int., 116, 286–299, https://doi.org/10.1016/j.envint.2018.04.018, 2018.

National Institute for Health Research: NIHR Funding and Awards Search Website, https://fundingawards.nihr.ac.uk/award/NIHR130095 (last access: 24 May 2022), 2020.

Oshiro, T. M., Perez, P. S., and Baranauskas, J. A.: How Many Trees in a Random Forest?, in: Machine Learning and Data Mining in Pattern Recognition, edited by: Perner, P., MLDM 2012, Lecture Notes in Computer Science, Vol. 7376, Springer, Berlin, Heidelberg, https://doi.org/10.1007/978-3-642-31537-4_13, 2012.

Probst, P., Wright, M., and Boulesteix, A.-L.: Hyperparameters and Tuning Strategies for Random Forest, https://wires.onlinelibrary.wiley.com/doi/10.1002/widm.1301 (last access: 24 May 2022), 2019.

Public Health England: Health matters: air pollution – GOV. UK, UK Gov., November, https://www.gov.uk/government/publications/health-matters-air-pollution/health-matters-air-pollution (last access: 24 May 2022), 2018.

Schneider, P., Castell, N., Vogt, M., Dauge, F. R., Lahoz, W. A., and Bartonova, A.: Mapping urban air quality in near real-time using observations from low-cost sensors and model information, Environ. Int., 106, 234–247, https://doi.org/10.1016/j.envint.2017.05.005, 2017.

Spinelle, L., Gerboles, M., and Aleixandre, M.: Performance evaluation of amperometric sensors for the monitoring of O_3 and NO_2 in ambient air at ppb level, Procedia Eng., 120, 480–483, https://doi.org/10.1016/j.proeng.2015.08.676, 2015.

Spinelle, L., Gerboles, M., Villani, M. G., Aleixandre, M., and Bonavitacola, F.: Field calibration of a cluster of low-cost commercially available sensors for air quality monitoring. Part B: NO, CO and CO_2, Sensor. Actuat. B-Chem., 238, 706–715, https://doi.org/10.1016/j.snb.2016.07.036, 2017a.

Spinelle, L., Gerboles, M., Kotsev, A., and Signorini, M.: Evaluation of low-cost sensors for air pollution monitoring: Effect of gaseous interfering compounds and meteorological conditions, JRC Technical Report, https://op.europa.eu/en/publication-detail/-/publication/23e1a2c7-3c41-11e7-a08e-01aa75ed71a1 (last access: 24 May 2022), 2017b.

De Vito, S., Piga, M., Martinotto, L., and Di Francia, G.: CO, NO_2 and NO_x urban pollution monitoring with on-field calibrated electronic nose by automatic bayesian regularization, ensor. Actuat. B-Chem., 143, 182–191, https://doi.org/10.1016/j.snb.2009.08.041, 2009.

Wang, S., Ma, Y., Wang, Z., Wang, L., Chi, X., Ding, A., Yao, M., Li, Y., Li, Q., Wu, M., Zhang, L., Xiao, Y., and Zhang, Y.: Mobile monitoring of urban air quality at high spatial resolution by low-cost sensors: impacts of COVID-19 pandemic lockdown, Atmos. Chem. Phys., 21, 7199–7215, https://doi.org/10.5194/acp-21-7199-2021, 2021.

Woodall, G., Hoover, M., Williams, R., Benedict, K., Harper, M., Soo, J.-C., Jarabek, A., Stewart, M., Brown, J., Hulla, J., Caudill, M., Clements, A., Kaufman, A., Parker, A., Keating, M., Balshaw, D., Garrahan, K., Burton, L., Batka, S., Limaye, V., Hakkinen, P., and Thompson, B.: Interpreting Mobile and Handheld Air Sensor Readings in Relation to Air Quality Standards and Health Effect Reference Values: Tackling the Challenges, Atmosphere, 8, 182, https://doi.org/10.3390/atmos8100182, 2017.

Yu, H., Lo, H., Hsieh, H., Lou, J., Mckenzie, T. G., Chou, J., Chung, P., Ho, C., Chang, C., Weng, J., Yan, E., Chang, C., Kuo, T., Chang, P. T., Po, C., Wang, C., Huang, Y., Ruan, Y., Lin, Y., Lin, S., Lin, H., and Lin, C.: Feature engineering and classifier ensemble for KDD Cup 2010, JMLR Work, Conf. Proc., http://citeseerx.ist.psu.edu/viewdoc/summary?doi=10.1.1.367.249 (last access: 4 May 2021), 2011.

Zhang, Z. M., Chen, S., and Liang, Y. Z.: Baseline correction using adaptive iteratively reweighted penalized least squares, Analyst, 135, 1138–1146, https://doi.org/10.1039/b922045c, 2010.

Zhang, Z. M., Chen, S., and Liang, Y. Z.: Google Code Archive – Long-term storage for Google Code Project Hosting, https://code.google.com/archive/p/airpls/ (last access: 5 May 2021), 2011.

Zimmerman, N., Presto, A. A., Kumar, S. P. N., Gu, J., Hauryliuk, A., Robinson, E. S., Robinson, A. L., and R. Subramanian: A machine learning calibration model using random forests to improve sensor performance for lower-cost air quality monitoring, Atmos. Meas. Tech., 11, 291–313, https://doi.org/10.5194/amt-11-291-2018, 2018.